Robust Estimator for Lens-based Hybrid MIMO with Low-Resolution Sampling

Evangelos Vlachos[1], John Thompson[1], Muhammad Ali Babar Abbasi[2], Vincent F. Fusco[2] and Michail Matthaiou[2]
[1]Institute for Digital Communications, University of Edinburgh, UK
[2] Institute of Electronics, Communications and Information Technology, Queen's University Belfast, UK
E-mails: {e.vlachos, j.s.thompson}@ed.ac.uk, {m.abbasi, v.fusco, m.matthaiou}@qub.ac.uk

***Abstract*—It is well known that large antenna arrays with beamforming capabilities are required to compensate for the high path-loss at millimeter-wave (mmWave) frequencies. Recently, a practical two-stage Rotman lens beamformer has demonstrated increased antenna gain with reduced implementation complexity, since the conventional beam selection network was omitted. In this work, we adopt this system and we investigate its performance in terms of symbol estimation when analog-to-digital converters (ADCs) with low-resolution sampling being employed. Although this design is characterized by low-complexity and low-cost, the analog beamformer and the ADCs introduce several impairments to the received signal. To mitigate these effects, we have developed a robust maximum a posteriori (MAP) estimator based on the Expectation-Maximization (EM) iterative algorithm. The proposed algorithm outperforms the conventional EM approach, exhibiting small mean-square-error in the medium to high signal-to-noise ratio regimes.**

I. Introduction

Multiple-input multiple-output (MIMO) wireless systems [1] provide higher capacity gains and a better reliability, while migration towards millimeter-wave (mmWave) frequencies will combat the lack of large bandwidth channels at conventional frequencies (i.e., below 6 GHz). However, in order to reap the real potential of mmWave MIMO systems a number of fundamental challenges have to be addressed. The high free space path-loss of a radio wave at mmWave frequencies requires compensation in terms of increased link gain. Beamforming is one of the prevalent concepts to achieve this. Hybrid transceiver architectures seem to be the most suitable, since they can provide low-cost mmWave radio front-end hardware. At mmWave frequencies, radio-frequency (RF) switches are generally *lossy* and their insertion loss tends to increase as the RF switches are cascaded to form a network. This degrades the overall system performance. Also due to the availability of only discrete switching devices, scalablity of the switching matrix to large array sizes is very difficult. In addition to this, the switching matrix at mmWave MIMO needs updating at every *coherence time* [1], which further increases the hardware complexity.

Lens based beamforming systems are found to be a practical alternative [2], [3], simplifying the mmWave MIMO radio frequency (RF) front-end. In this context, one classical approach of such is the use of single stage Rotman lens connected to an antenna array. A recent development of this for 28 GHz communication can be found in [4] and the references therein. A Rotman lens comprises of a wave propagation medium with beam ports and array ports. Wave propagation inside the lens with phase differences defines the tilt of a beam. ARotman lens with a compact antenna array and integrated amplifiers at 60 GHz is also shown to be capable of beam-steering and active beam-switching at the same time [2]. A thorough investigation of Rotman lens based MIMO systems with beam selection and digital beamforming can be found in [5]. Recently, a practical two-stage Rotman lens analog beamformer has demonstrated increased antenna gain with reduced implementation complexity, since the conventional beam selection network was omitted [6]. In addition, high fidelity specifications considering the sampling resolution of the analog-to-digital converters (ADCs) have been alleviated, and designs with lower resolution ADCs are being proposed [7]. In particular, since ADCs have large power consumption, lowering their resolution significantly reduces the overall system power consumption and hardware complexity, at the expense of the introduced distortion to the received signal. The effect of low resolution ADCs on channel capacity has been studied for MIMO channels in [8], [9].

Contributions: We consider a hybrid MIMO receiver where the analog part is composed by a two-stage stacked lens architecture (Fig. 1). The analog and digital parts are connected by a number of RF chains L_{R} which is less than the number of antenna elements N_{R}. The output of each RF chain is connected to a low-resolution ADC, before the baseband processing step. Note that, this system performs lens-based analog phase shifting and does not include the RF switching stage. This design provides a tradeoff between hardware complexity and introduced noise to the received signal. To mitigate this effect, we develop a robust Expectation-Maximization (EM) technique which is able to perform better than the conventional approaches in the mid to high signal-to-ratio (SNR) regimes. The main idea is to model a part of the input as noise with known statistics. The proposed technique is able to estimate this noise and remove it from the received signal. This is verified via extensive simulation results, which show that the

The authors gratefully acknowledge funding of this work by EPSRC grants EP/P000703/1, EP/P000673/1 and EP/P000391/1.

978-1-5386-6528-2/19/$31.00 ©2019 IEEE

mean-square-error (MSE) of the robust EM estimator is lower than the conventional EM approach.

Notation: $\mathbf{A}$, $\mathbf{a}$, and a denote a matrix, a vector, and a scalar, respectively. The complex conjugate transpose, and transpose of $\mathbf{A}$ are denoted as $\mathbf{A}^H$ and $\mathbf{A}^T$; $\mathbf{I}_N$ represents $N \times N$ identity matrix; $\mathbf{X} \in \mathbb{C}^{A\times B}$ and $\mathbf{X} \in \mathbb{R}^{A\times B}$ denote an $A \times B$ size $\mathbf{X}$ matrix with complex and real entries, respectively; $\mathcal{CN}(\mathbf{a}; \mathbf{A})$ denotes a complex Gaussian vector having mean $\mathbf{a}$ and covariance matrix $\mathbf{A}$; the expectation of a complex variable is denoted as $\mathcal{E}\{\cdot\}$; $[\mathbf{A}]_k$ denotes the k-th column of matrix $\mathbf{A}$ and $[\mathbf{A}]_{kl}$ is the matrix entry at the k-th row and l-th column.

II. System Model

A. MmWave Channel Model

Let us consider a receiver with antenna array size equal to M. The $M \times 1$ uplink channel vector for the ℓ–th terminal is modeled as a *double–directional* response consisting of a finite number of multipath components (MPCs) [10],

$$\mathbf{h}_\ell = \frac{1}{\sqrt{N_{\mathrm{P}}}} \sum_{p=1}^{N_{\mathrm{P}}} \alpha_{\ell,p}\, \Lambda\left(\phi_{\ell,p}, \theta_{\ell,p}\right) \mathbf{a}^H(\phi_{\ell,p}, \theta_{\ell,p}), \quad (1)$$

where N_{P} is the number of MPCs, while $\alpha_{\ell,p}$ models the path gains of the p–th MPC, $\Lambda\left(\phi_{\ell,p}, \theta_{\ell,p}\right)$ denotes the per–antenna element gain, while $\mathbf{a}\left(\phi_{\ell,p}, \theta_{\ell,p}\right)$ is the far–field steering vector of the uniform rectangular array (URA) [11]. Also, $\alpha_{\ell,p} \sim \mathcal{CN}\left(0, \beta_\ell\right)$ where $\beta_\ell = \zeta_\ell (r_{\mathrm{ref}}/r_\ell)^\chi$ captures the large–scale fading impact within the channel, including the shadow fading and geometric attenuation with the distance r_ℓ from the ℓ-th UE to the URA. In particular, $10\log_{10}(\zeta_\ell) \sim \mathcal{CN}\left(0, \sigma_{\mathrm{sf}}^2\right)$, where σ_{sf} is the standard deviation of the shadow fading. Here, r_{ref} is the reference distance from URA, while χ is the path-loss attenuation exponent.

B. Two-stage Rotman-lens Beamformer

We consider a basestation (BS) equipped with a URA followed by a two–stage Rotman lens–based beamformer. Diverging from the classical MIMO architectures, in which each antenna element is required to have its own RF chain to connect to the base-band processing unit: the number of antennas used in this topology is 15 while the number of RF chains is 9[1]. The $L \times 1$ down–converted signal $\mathbf{y} \in \mathbb{C}^{L\times 1}$ can be written as:

$$\mathbf{y} = \rho^{1/2} \mathbf{F}_{\mathrm{RF}} \mathbf{H} \mathbf{s} + \mathbf{n} \quad (2)$$

where $\mathbf{s} \in \mathbb{C}^{L\times 1}$ is the $L \times 1$ vector with the transmitting symbols from all terminals, $\mathbf{H} \in \mathbb{C}^{N_{\mathrm{R}}\times L}$ is the mmWave channel matrix, $\mathbf{F}_{\mathrm{RF}} \in \mathbb{C}^{L\times N_{\mathrm{R}}}$ is the lens-based beamformer matrix and $\mathbf{n} \in \mathbb{C}^{L\times 1}$ is the additive complex Gaussian noise vector with $\mathbf{n} \sim \mathcal{CN}(\mathbf{0}, \sigma_n^2 \mathbf{I}_L)$. We assume that the beamformer is capable of creating M fixed analog beams along the azimuth and elevation sectors as $(\phi_1, \theta_1), \ldots, (\phi_M, \theta_M)$. The net functionality of the lens–based beamformer when considering a perfect focusing capability is described by the $L \times M$ matrix:

$$\mathbf{F}_{\mathrm{RF}} = \left[\mathbf{a}^H(\phi_1, \theta_1)\ \mathbf{a}^H(\phi_2, \theta_2)\ \ldots\ \mathbf{a}^H(\phi_M, \theta_M)\right]^T. \quad (3)$$

C. Low-resolution Quantization

As shown in Fig. 1, the outputs of the 2D Rotman-lens beamformer are connected to L parallel RF chains which represent the received complex signal vector $\mathbf{y} \in \mathbb{C}^{L\times 1}$. This signal passes through L ADCs with low-resolution quantization, i.e., $b \in \{3, \ldots, 7\}$ bits for each real or imaginary component. This bit range provides an acceptable compromise between the power requirements and the performance reduction. Hence,

$$\mathbf{r} = \mathcal{Q}\big(\mathtt{Re}(\mathbf{y})\big) + j\mathcal{Q}\big(\mathtt{Im}(\mathbf{y})\big) \quad (4)$$

where $\mathcal{Q}(\cdot)$ represents a uniform symmetric mid-riser type quantizer which is applied independently at each component of the input vector. Specifically, for the scalar input x it is defined as:

$$\mathcal{Q}(x) = \mathrm{sign}(x) \left[\min\left(\left\lceil \frac{|x|}{\delta} \right\rceil, 2^{b-1}\right) - \frac{1}{2}\right] \delta \quad (5)$$

where $\delta \triangleq \left(\mathcal{E}(|x|^2)\right)^{1/2}\gamma$ and γ is the quantization stepsize. We assume that the average power $\mathcal{E}(|x|^2)$ is known, measured by an automatic gain control unit, while the stepsize γ is chosen optimally so as to minimize the quantization error assuming a Gaussian input signal [12].

III. Proposed Robust Estimator

A. Problem Formulation

The two–stage stacked Rotman lens–based beamformer eliminates the requirement of a switching matrix by carefully adding capability inside the beamformer [6]. However, closely spaced antenna elements are subject to mutual coupling that has a negative impact on per antenna element efficiency. Also, the Rotman lens has its own inherent losses (see [13], [14] for details). We have measured the realistic beam patterns for the Rotman lens system in an anechoic chamber (see Fig. 2). Thus, we model these imperfections of the antenna and the beamformer according to:

$$\mathbf{F}_{\mathrm{RF}} = \mathbf{F}_{\mathrm{RF}}^o + \mathbf{E} \quad (6)$$

where the matrix $\mathbf{E} \in \mathbb{C}^{L\times N_{\mathrm{R}}}$ represents the distortion due to beamformer and antenna design imperfections and $\mathbf{F}_{\mathrm{RF}}^o$ is the ideal beamforming matrix.

Then, the received signal $\mathbf{r}$, measured at the outputs of the ADCs is expressed as:

$$\mathbf{r} = \mathcal{Q}(\mathbf{y}) = \mathcal{Q}(\mathbf{F}_{\mathrm{RF}}\mathbf{H}\mathbf{s} + \mathbf{n}) = \mathcal{Q}(\mathbf{F}_{\mathrm{RF}}^o\mathbf{H}\mathbf{s} + \mathbf{E}\mathbf{H}\mathbf{s} + \mathbf{n}) \quad (7)$$

$$= \mathcal{Q}(\underbrace{\mathbf{F}_{\mathrm{RF}}^o\mathbf{H}}_{\mathbf{\Psi}}\mathbf{s} + \mathbf{d} + \mathbf{n}) \quad (8)$$

where $\mathbf{d} \in \mathbb{C}^{L\times 1}$ represents the *beamforming noise* and $\mathbf{\Psi} \triangleq \mathbf{F}_{\mathrm{RF}}^o\mathbf{H}$. Hence, the output can be expressed as the signal plus two noise vectors, i.e., $\mathbf{d}+\mathbf{n}$. In general, the beamforming noise vector $\mathbf{d}$ is unknown, since we have no knowledge of

[1]Minimum number of beam ports (N_{bp}) a Rotman lens can support is 3. Our proof–of–concept hardware thus contained 3 ports for each of the 3 Rotman lenses making overall 9 input ports. Number of antenna elements was selected to proof that the proposed architecture can reduce the number of active RF–chains by supporting a higher number of antenna elements, i.e. 15 (3 Rotman lenses with N_{ap} = 5) using a lower inputs, i.e. 9.

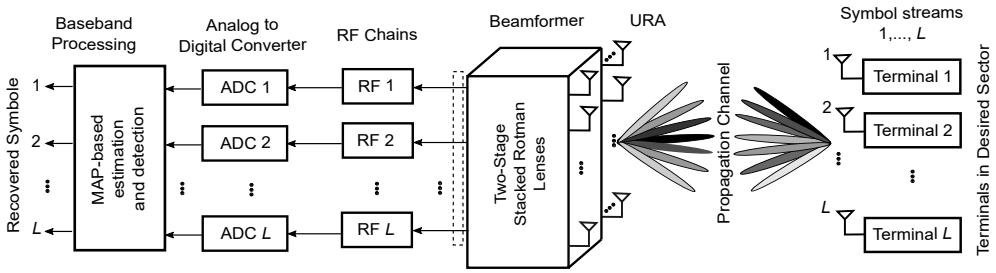

Fig. 1. MU-MIMO uplink system model with a two–stage Rotman lens–based hybrid beamformer and low–resolution ADC per RF chain.

the noise matrix $\mathbf{E}$. In this work, we will assume that $\mathbf{d}$ is a Gaussian random variable with covariance matrix $\sigma_d^2\mathbf{I}_L$. Therefore, the value of σ_d^2 has to carefully selected because it will have an impact on the estimation performance.

It is well known that the quantization function $\mathcal{Q}(\cdot)$ is a non-linear function and therefore difficult to analyze directly. This makes the simple linear estimators (e.g., linear miminum mean square estimator - LMMSE) inappropriate, resulting in high estimation errors. However, working on the statistical properties of the quantized signal allows *strictly linear operations* to be performed [15]. To this end, we focus on the maximum a-posteriori (MAP) estimator, which can be expressed as:

$$(\tilde{\mathbf{s}}, \tilde{\mathbf{d}}) = \arg\max_{\mathbf{s},\mathbf{d}} p(\mathbf{r}, \mathbf{y}, \mathbf{d}, \mathbf{s}) \tag{9}$$

with $p(\mathbf{r}, \mathbf{y}, \mathbf{d}, \mathbf{s})$ being the joint PDF of the quantized output, the received signal, the unknown noise and the transmitted symbols.

B. Robust Expectation-Maximization Estimator

Next, we describe a maximum a-posteriori (MAP) estimator to obtain the transmitted symbols $\mathbf{s}$. The proposed technique is based on the Expectation-Maximization (EM) algorithm [16] which approximates the MAP solution. Specifically, EM is an iterative method that tries to find the maximum likelihood estimator of a parameter $\mathbf{s}$ of a parametric probability distribution $\mathbf{p}(\mathbf{r}|\mathbf{s})$. The quantities $\mathbf{y}$ and $\mathbf{d}$ are considered as unknown and they are calculated by the EM technique [17].

Proposition 1. *The Expectation-Maximization algorithm which solves* (9) *is described by the following steps for the* $(m+1)$*-th iteration:*

- ***E-step***
  Compute the vector $\mathbf{b}^{(m+1)} \in \mathbb{R}^{2L\times 1}$ *with*

$$[\mathbf{b}^{(m+1)}]_i = -\frac{\sigma_n}{\sqrt{2\pi}} \frac{\xi(l_i) - \xi(u_i)}{\Xi(l_i) - \Xi(u_i)} \tag{10}$$

  where l_i, u_i *are the lower/upper bounds of the quantizer for* $[\mathbf{r}]_i$ *respectively;*

$$\xi(a) \triangleq e^{-\frac{(a-[\mathbf{\Psi}\mathbf{s}^{(m)}]_i - [\mathbf{d}]_i)^2}{2\sigma^2}},$$

$$\Xi(a) \triangleq \text{erf}\left(\frac{-a + [\mathbf{\Psi}\mathbf{s}^{(m)}]_i + [\mathbf{d}]_i}{\sqrt{2}\sigma_n}\right),$$

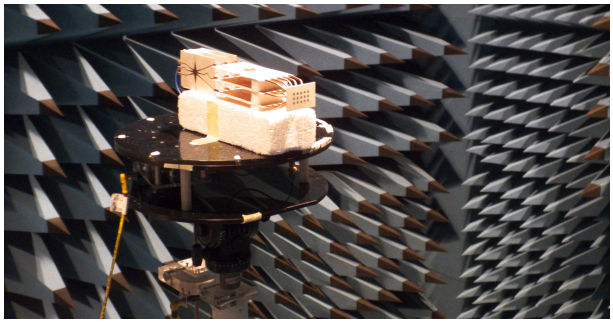

Fig. 2. Measurement setup in NSI anechoic chamber at Queen's University, Belfast. Photographs were taken before covering the Rotman lens layers with absorbers.

  with $\text{erf}(\cdot)$ *is the error function.*

- ***M-step***
  - *Estimate the symbols vector* $\mathbf{s}^{(m+1)} \in \mathbb{R}^{2L\times 1}$ *by solving the linear system of equations:*

$$\mathbf{A}\mathbf{s}^{(m+1)} = \mathbf{\Psi}^T\mathbf{c} \tag{11}$$

    where

$$\mathbf{A} \triangleq \mathbf{\Psi}^T\mathbf{\Psi} + \sigma_n^2\mathbf{I}_L,$$

$$\mathbf{c} \triangleq \mathbf{\Psi}\mathbf{s}^{(m)} + \mathbf{b}^{(m+1)} + \mathbf{d}^{(m)}$$

  - *Obtain the update of the noise vector:*

$$\mathbf{d}^{(m+1)} = \sigma_d^2\mathbf{\Psi}\mathbf{s}^{(m+1)} \tag{12}$$

Proof: See Appendix. VI.

The computational complexity order of the EM algorithm is mainly determined by the complexity of equation (11). The complexity order of (10) and (12) is only $\mathcal{O}(M)$ while the number of the iterations which are required for convergence is usually very small (e.g., 10-20).

IV. Performance Evaluation

A. Beamformer Characteristics

The two stages of the lens are constructed using stacked printed circuit boards (PCBs) with one side grounded and the other side containing the lens structure. The simulated and fabricated prototype is presented in Fig. 3. We used the classical Rotman lens principles to design all the lenses. The first stage lens, i.e. right after the URA, consists of $N_{\text{ap}} = 5$ and $N_{\text{bp}} = 3$,

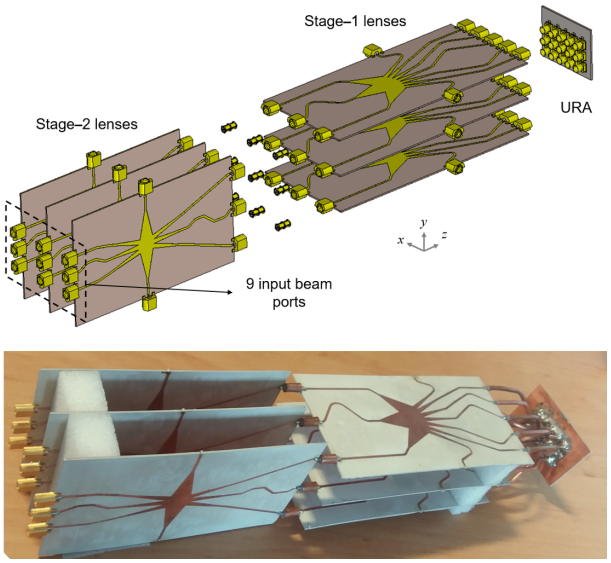

Fig. 3. Simulated structural configuration and developed hardware [6], [14] of the two–stage Rotman lens–based beamformer.

followed by the second stage lens having $N_{\text{ap}} = N_{\text{bp}} = 3$. The first stage lens is implemented for beamfoming along azimuth, while the second stage lenses handle beamforming in elevation. The URA antenna elements are operational at 28 GHz, having a -10dB return loss bandwidth of 3650 MHz. The antennas are fabricated using the LPKF H100 milling machine using microstrip technology. The tri-focal Rotman lens synthesis method, as described in the classical literature [18] is used to develop the lenses. The on-axis focal length $f_1 = 3\lambda$, an on and off–axis focus length ratio $\beta = 0.9$ is considered for the first stage lenses. In addition, the focal angle α is $30°$, the sweep angle φ_{max} is $40°$, while the array steering angle ϕ is $40°$. Similarly, the parameters set for the second stage lens are: $f_1 = 2\lambda$, $\beta = 0.95$, $\alpha = 30°$, $\varphi_{\text{max}} = 30°$ and the steering range is $\theta = 15°$. In both lens stages, tapering lines are used to connected the lens internal structure to the 50Ω transmission lines. All tapering lines are 3λ in length. Note that it is important that all lines connecting the lens structure to the edge of the PCB need to be phase aligned.

B. Estimation Performance

In this subsection, we evaluate the performance of the proposed technique via computer simulations. All the results have been averaged over $1,000$ Monte-Carlo realizations. The mmWave channel was simulated at 28GHz assuming 4 scattering clusters with a total number of 5 sub-paths for each cluster. The instantaneous path gains were modeled based on Gaussian distribution with zero-mean and unit variance. The UE transmit L Gaussian symbols with repetition coding of length T. The average transmit power was set to $\rho^{1/2} = 0.1$. We have considered the range of 3-5 bit resolutions for the ADCs.

We compare the performance of the proposed estimator (Robust-EM) with the conventional EM estimator [16] and

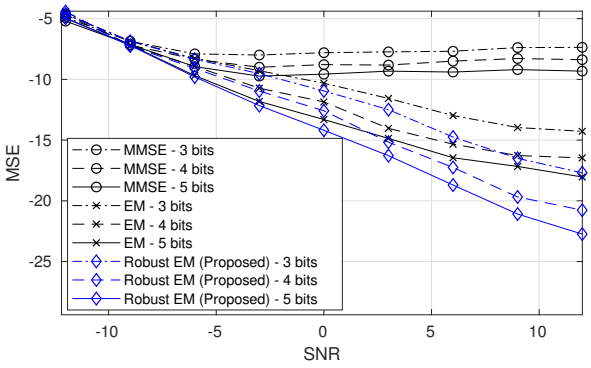

Fig. 4. Mean square error of the lens-based geometry w.r.t. SNR, with $T = 100$ and $\sigma_d^2 = 0.012$.

minimum mean square estimator (MMSE). The results are shown in Fig. 4 for the cases of 3, 4 and 5 bit ADC resolution. We observe that MMSE is not able to achieve lower than -10dB mean-square-error (MSE), for all cases. Also, EM performs better than MMSE, since it takes into account the low-resolution quantization, however, due to beamforming impairments is not able to reach below -17dB MSE. The proposed Robust EM techniques achieves lower than -20dB even with only 4 bits ADC resolution.

The MSE with respect to the length of the repetition coding is investigated in Fig. 5(a). All the considered techniques require at least 50 repetitions to reach their best MSE level. The remaining error is due to the low-resolution quantization, which cannot be alleviated with the simple scheme of repetition. The impact of the beamforer error variance σ_d^2 on the performance of the proposed technique is shown in Fig. 5(b). We plot the MSE when the ADC resolution is 3,4 and 5 bits. Note that MSE is not decreasing monotonically over σ_d^2 and the lowest value is achieved when $\sigma_d^2 \in (0.01, 0.015)$. This range indicates the set of optimal modeling parameters for the second order statistics of the unknown noise vector $\mathbf{d}$.

We also consider the case where the UE transmits 4-QAM symbols, where at the receiver, symbol detection is implemented after obtaining the soft-desicions. The results are presented in Fig. 6 for the case of $T = 20$. The results validate the robustness of the proposed technique to the signal impairments of the Rotman lens system.

V. Conclusions

We have considered a hybrid MIMO receiver with two-stage stacked lens architecture and low-resolution ADCs. The analog part of this system does not include the RF switching stage. This design provides a tradeoff between the hardware complexity and the introduced noise to the received signal. We have developed a robust maximum a posteriori (MAP) estimator based on Expectation-Maximization (EM) iterative algorithm, which outperforms the conventional EM approach in terms of MSE and symbol error rate. This is achieved without increasing the hardware complexity of the system,

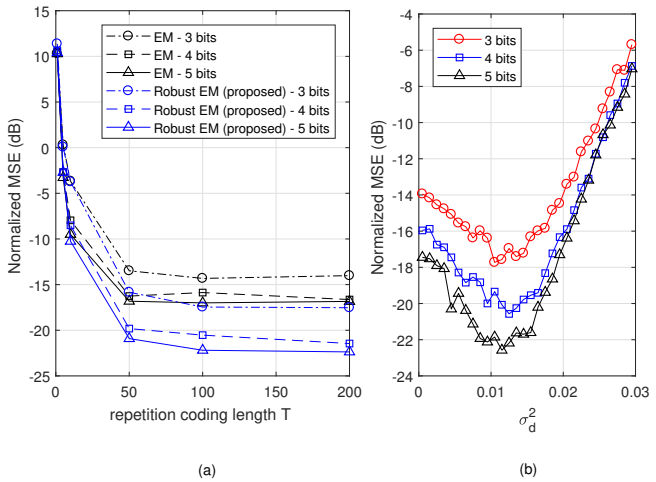

Fig. 5. (a) MSE w.r.t. repetition coding length T, (b) MSE w.r.t. beamformer noise variacne σ_d^2 with SNR=15dB.

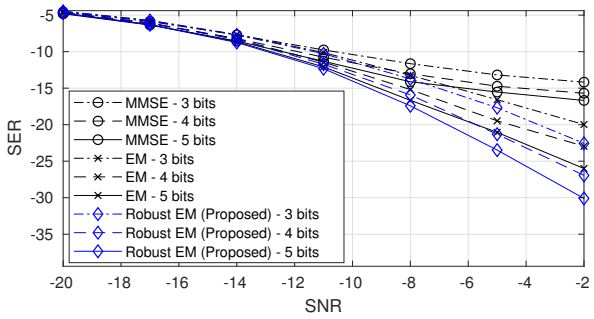

Fig. 6. Symbol-error-rate w.r.t. SNR with $T = 20$ and $\sigma_d^2 = 0.012$.

while the baseband signal processing complexity increases only slightly.

VI. Appendix:Proof of Proposition 1

The joint PDF can be written as: $p(\mathbf{r},\mathbf{y},\mathbf{d},\mathbf{s}) = p(\mathbf{r}|\mathbf{y})p(\mathbf{y}|\mathbf{d},\mathbf{s})p(\mathbf{d})p(\mathbf{s})$. Hence, taking the expectation over the unknown variables we have $\mathcal{E}_{\mathbf{y},\mathbf{d}|\mathbf{r},\mathbf{s}^{(m)}}\{\ln p(\mathbf{r},\mathbf{y},\mathbf{d},\mathbf{s})\} = \mathcal{E}_{\mathbf{y},\mathbf{d}|\mathbf{s}^{(m)}}\{\ln p(\mathbf{y}|\mathbf{d},\mathbf{s})\} + \ln p(\mathbf{r}|\mathbf{y}) + \mathcal{E}_{\mathbf{d}|\mathbf{r},\mathbf{s}^{(m)}}\{\ln p(\mathbf{d})\} + \ln p(\mathbf{s})$. The first term can be written as: $\mathcal{E}_{\mathbf{y},\mathbf{d}|\mathbf{s}^{(m)}}\{\ln p(\mathbf{y}|\mathbf{d},\mathbf{s})\} = -\frac{1}{2\sigma_n^2}\mathcal{E}\left\{\|\mathbf{y}-\mathbf{\Psi}\mathbf{s}-\mathbf{d}\|_2^2\right\} + \kappa_1$, with κ_1 a constant term. The expectation term is further expanded as $\mathcal{E}_{\mathbf{y},\mathbf{d}|\mathbf{s}^{(m)}}\left\{\|\mathbf{y}-\mathbf{\Psi}\mathbf{s}-\mathbf{d}\|_2^2\right\} = \mathcal{E}_{\mathbf{y},\mathbf{d}|\mathbf{s}^{(m)}}\left\{\|\mathbf{y}-\mathbf{d}\|_2^2\right\} - 2\mathcal{E}_{\mathbf{y},\mathbf{d}|\mathbf{s}^{(m)}}\left\{(\mathbf{y}-\mathbf{d})^T\mathbf{\Psi}\mathbf{s}\right\} + \|\mathbf{\Psi}\mathbf{s}\|_2^2$. Keeping only the terms that depend on $\mathbf{s}$ and $\mathbf{d}$ we define the function:

$$\mathcal{G} \triangleq -\frac{1}{2\sigma_n^2}\left(-2\mathcal{E}_{\mathbf{y},\mathbf{d}|\mathbf{s}^{(m)}}\left\{(\mathbf{y}-\mathbf{d})^T\mathbf{\Psi}\mathbf{s}\right\} + \|\mathbf{\Psi}\mathbf{s}\|_2^2 + \mathcal{E}_{\mathbf{y},\mathbf{d}|\mathbf{s}^{(m)}}\left\{-2\mathbf{y}^T\mathbf{d} + \|\mathbf{d}\|_2^2\right\}\right) + \ln p(\mathbf{s}) \quad (13)$$

$$= \frac{1}{2\sigma_n^2}\left(2\mathcal{E}_{\mathbf{y},\mathbf{d}|\mathbf{s}^{(m)}}\{\mathbf{y}\}^T\mathbf{\Psi}\mathbf{s} + 2\mathbf{d}^T\mathbf{\Psi}\mathbf{s} - \|\mathbf{\Psi}\mathbf{s}\|_2^2 - \|\mathbf{d}\|_2^2 + 2\mathcal{E}_{\mathbf{y},\mathbf{d}|\mathbf{s}^{(m)}}\{\mathbf{y}\}^T\mathbf{d}\right) - \frac{1}{2\sigma_s^2}\|\mathbf{s}\|_2^2 \quad (14)$$

where (14) represents the mean of the truncated Gaussian random variable. Hence,

$$\mathcal{E}_{\mathbf{y},\mathbf{d}|\mathbf{s}^{(m)}}\{[\mathbf{y}]_i\} = [\mathbf{\Psi}\mathbf{s}^{(m)}]_i + \sigma_n\frac{\xi(r_i^{\text{lo}}) - \xi(r_i^{\text{up}})}{\Xi(r_i^{\text{up}}) - \Xi(r_i^{\text{lo}})}. \quad (15)$$

Taking the derivative of $\mathcal{G}$ over $\mathbf{s}$ and setting it equal to zero, we have $\frac{\partial\mathcal{G}}{\partial\mathbf{s}} = \mathbf{0} \Rightarrow 2\mathbf{\Psi}^T\mathbf{c} - 2(\mathbf{\Psi}^T\mathbf{\Psi} + \frac{\sigma_n^2}{\sigma_s^2})\mathbf{s} = \mathbf{0}$ where $\mathbf{c} \triangleq [\mathbf{\Psi}\mathbf{s}^{(m)}]_i + \sigma_n\frac{\xi(r_i^{\text{lo}})-\xi(r_i^{\text{up}})}{\Xi(r_i^{\text{up}})-\Xi(r_i^{\text{lo}})} - \mathbf{d}$. Finally, taking the derivative of $\mathcal{G}$ over $\mathbf{d}$ and setting it equal to zero, we have $\frac{\partial\mathcal{G}}{\partial\mathbf{d}} = \mathbf{0} \Rightarrow \mathbf{d} = \sigma_d^2\mathbf{\Psi}\mathbf{s}$.

References

[1] E. G. Larsson, T. L. Marzetta, H. Q. Ngo, and H. Yang, "Antenna count for massive MIMO: 1.9 GHz vs. 60 GHz," *IEEE Commun. Mag.*, vol. 56, no. 9, pp. 132–137, Sep. 2018.

[2] W. H. *et al.*, "Multibeam antenna technologies for 5G wireless communications," *IEEE Trans. Ant. Propag.*, vol. 65, no. 12, pp. 6231–6249, Dec 2017.

[3] M. A. B. Abbasi, V. F. Fusco, H. Tataria, and M. Matthaiou, "Constant-ϵ_r lens beamformer for low-complexity millimeter-wave hybrid MIMO," *IEEE Trans. Microw. Theory Tech.*, pp. 1–10, 2019.

[4] E. H. Mujammami, I. Afifi, and A. B. Sebak, "Optimum wideband high gain analog beamforming network for 5G applications," *IEEE Access*, vol. 7, pp. 52 226–52 237, 2019.

[5] Y. Gao, M. Khaliel, F. Zheng, and T. Kaiser, "Rotman lens based hybrid analogdigital beamforming in massive MIMO systems: Array architectures, beam selection algorithms and experiments," *IEEE Trans. Veh. Technol.*, vol. 66, no. 10, pp. 9134–9148, Oct 2017.

[6] M. A. B. Abbasi, H. Tataria, V. F. Fusco, and M. Matthaiou, "Performance of a 28 GHz two-stage rotman lens beamformer for millimeter wave cellular systems," in *Proc. IEEE EuCAP*, Apr. 2019.

[7] S. Jacobsson, G. Durisi, M. Coldrey, U. Gustavsson, and C. Studer, "Throughput analysis of massive MIMO uplink with low-resolution ADCs," *IEEE Trans. Wireless Commun.*, vol. 16, no. 6, pp. 4038–4051, Jun. 2017.

[8] J. Mo, A. Alkhateeb, S. Abu-Surra, and R. W. Heath, "Hybrid architectures with few-bit ADC receivers: achievable rates and energy-rate tradeoffs," *IEEE Trans. Wireless Commun.*, vol. 16, no. 4, pp. 2274–2287, Apr. 2017.

[9] J. Mo, P. Schniter, and R. W. Heath, "Channel estimation in broadband millimeter wave MIMO systems with few-bit ADCs," *IEEE Trans. Signal Process.*, vol. 66, no. 5, pp. 1141–1154, Mar. 2018.

[10] A. F. Molisch, V. V. Ratnam, S. Han, Z. Li, S. L. H. Nguyen, L. Li, and K. Haneda, "Hybrid beamforming for massive MIMO: A survey," *IEEE Commun. Mag.*, vol. 55, no. 9, pp. 134–141, Sep. 2017.

[11] W. Tan, S. D. Assimonis, M. Matthaiou, Y. Han, X. Li, and S. Jin, "Analysis of different planar antenna arrays for mmWave massive MIMO systems," in *Proc. IEEE VTC*, June 2017, pp. 1–5.

[12] J. Max, "Quantizing for minimum distortion," *IRE Transactions on Information Theory*, vol. 6, no. 1, pp. 7–12, March 1960.

[13] M. A. B. Abbasi, H. Tataria, V. F. Fusco, and M. Matthaiou, "On the impact of spillover losses in 28 GHz Rotman lens arrays for 5G applications," in *2018 IEEE IMWS-5G*, Aug 2018, pp. 1–3.

[14] M. A. B. Abbasi, V. F. Fusco, H. Tataria, and M. Matthaiou, "Lensbased beamformer for low-complexity millimeterwave cellular systems," in *Proc. ESA Workshop on Millimetre-Wave Technology and Applications*, Dec 2018.

[15] B. Widrow and I. Kollár, *Quantization Noise: Roundoff Error in Digital Computation, Signal Processing, Control, and Communications* . Cambridge, UK: Cambridge University Press, 2008.

[16] M. R. Gupta and Y. Chen, "Theory and use of the EM algorithm," *Found. Trends Signal Process.*, vol. 4, no. 3, pp. 223–296, Mar. 2011.

[17] A. Mezghani, F. Antreich, and J. A. Nossek, "Multiple parameter estimation with quantized channel output," in *Proc. ITG WSA*, Feb. 2010, pp. 143–150.

[18] R. C. Hansen, "Design trades for Rotman lenses," *IEEE Trans. Ant. Propag.*, vol. 39, no. 4, pp. 464–472, Apr. 1991.